

Enhancing interfacial conductivity and spatial charge confinement of LaAlO₃/SrTiO₃ heterostructures via strain engineering

Safdar Nazir, Maziar Behtash, and Kesong Yang

Citation: [Applied Physics Letters](#) **105**, 141602 (2014); doi: 10.1063/1.4897626

View online: <http://dx.doi.org/10.1063/1.4897626>

View Table of Contents: <http://scitation.aip.org/content/aip/journal/apl/105/14?ver=pdfcov>

Published by the [AIP Publishing](#)

Articles you may be interested in

[Electronic and magnetic phenomena at the interface of LaAlO₃ and Ru doped SrTiO₃](#)

Appl. Phys. Lett. **107**, 241603 (2015); 10.1063/1.4938133

[Compositional and gate tuning of the interfacial conductivity in LaAlO₃/LaTiO₃/SrTiO₃ heterostructures](#)

Appl. Phys. Lett. **102**, 091601 (2013); 10.1063/1.4794410

[Controlling interfacial states in amorphous/crystalline LaAlO₃/SrTiO₃ heterostructures by electric fields](#)

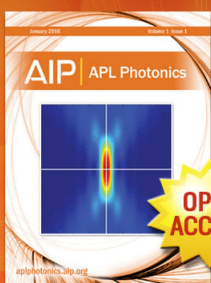
Appl. Phys. Lett. **102**, 021602 (2013); 10.1063/1.4775669

[Uniaxial strain-modulated conductivity in manganite superlattice \(LaMnO₃ / SrMnO₃ \)](#)

Appl. Phys. Lett. **98**, 031910 (2011); 10.1063/1.3548675

[Photovoltaic effect in the La_{0.67}Ca_{0.33}MnO₃ / LaMnO₃ / SrTiO₃ : Nb heterojunctions with variant LaMnO₃ layers](#)

Appl. Phys. Lett. **95**, 052502 (2009); 10.1063/1.3194776



Launching in 2016!
The future of applied photonics research is here

AIP | APL
Photonics

Enhancing interfacial conductivity and spatial charge confinement of $\text{LaAlO}_3/\text{SrTiO}_3$ heterostructures via strain engineering

Safdar Nazir, Maziar Behtash, and Kesong Yang^{a)}

Department of NanoEngineering, University of California, San Diego, 9500 Gilman Drive, Mail Code 0448, La Jolla, California 92093-0448, USA

(Received 11 August 2014; accepted 27 September 2014; published online 8 October 2014)

We explored the possibility of enhancing interfacial conductivity and spatial charge confinement of $\text{LaAlO}_3/\text{SrTiO}_3$ (LAO/STO) heterostructure (HS) via **strain engineering using first-principles** electronic structure calculations. We found that applying a tensile strain on the STO substrate along the *ab*-plane can significantly enhance the interfacial conductivity, magnetic moments, and the spatial charge confinement of the HS system. In contrast, a compressive strain can dilute the interfacial charge carrier density, make the mobile charges transfer to deep STO substrate, and weaken the spatial charge confinement along the *c*-axis. Hence, we propose that applying a tensile strain can be an effective way to enhance the interfacial conductivity and magnetism of STO-based HS systems.
 © 2014 AIP Publishing LLC. [<http://dx.doi.org/10.1063/1.4897626>]

The highly mobile two-dimensional electron gas (2DEG) formed on the polar/non-polar $\text{LaAlO}_3/\text{SrTiO}_3$ (LAO/STO) heterostructure (HS) is a matter of great interest because of its potential applications in next-generation nanoelectronic devices.^{1–5} The 2DEG formed on the LAO/STO HS has a large carrier density ($\sim 10^{13} \text{ cm}^{-2}$) and high carrier mobility ($\sim 10^4 \text{ cm}^2 \text{ V}^{-1} \text{ s}^{-1}$), showing superior transport properties.^{1,4,6} Moreover, the 2DEG can exhibit tunable electronic and magnetic properties,^{7–10} which provides promising prospects for enhancing the functionality of nanoelectronic devices. An ideal 2DEG can move freely in two dimensions along the interface, but is tightly confined in the third direction. However, in real interface materials such as LAO/STO, the 2DEG is extended to the third dimension, i.e., perpendicular to the interface, along the *c*-axis up to 20 Å,^{6,11} and thus it is also called quasi-2DEG.⁵ This extension can decentralize the occupation of 3*d* orbitals of the interfacial Ti ions in *ab*-plane, and hence reduce the interfacial charge carrier density and mobility of the 2DEG. This is detrimental to the performance of low-dimensional nanoelectronic devices. To make 2DEG systems suitable for high-performance nanoelectronics, it is therefore necessary to enhance their charge confinement and interfacial charge carrier density.

A lattice-mismatch-induced strain on an epitaxially grown film often has a significant influence on the electronic properties of the film. For instance, an ordinary band insulator consisting of heavy elements may become a topological insulator under an appropriate strain.¹² However, the lattice-mismatch-induced strain is mostly exerted on the deposited film instead of the substrate, i.e., STO. For the LAO/STO HS system, it is widely accepted that a charge transfer from the polar LAO to non-polar STO induced by the so-called “*polar catastrophe*” mechanism leads to the interfacial conductivity via partially occupied Ti 3*d* orbitals.^{2,13,14} In other words, the 2DEG is mainly induced by the Ti atoms of the STO substrate rather than the deposited perovskite oxide. Hence,

such lattice-mismatch-induced strains, occurring within the deposited perovskite oxide, cannot improve the electronic properties of STO-based 2DEG systems. Therefore, one may speculate that applying a strain on the STO substrate can be an effective way to modify the electric properties of the 2DEG system. In spite of the practical difficulty of applying a strain on the STO substrate of the LAO/STO HS system, one possible strategy to achieve this goal can be realized by two sequence steps, as shown in a previous experiment.¹⁵ First, the STO can be grown on an appropriate single-crystal substrate with a different lattice constant. Next, the LAO film can be deposited on the STO substrate to form the HS.

In this letter, we explored the possibility of enhancing the interfacial charge carrier confinements via strain engineering from first-principles electronic structure calculations. We analyzed the influence of the biaxial compressive and tensile strain on the interfacial charge carrier density, magnetic moments, and charge confinement effects of $(\text{LaO})^{+1}/(\text{TiO}_2)^0$ *n*-type LAO/STO HS. We propose that applying a tensile strain on the STO substrate along the *ab*-plane can effectively optimize the interfacial conductivity, magnetic moments, and the spatial charge confinement of the STO-based 2DEG system.

Our spin-polarized density functional theory electronic structure calculations were performed using the Vienna *Ab-initio* Simulation Package (VASP),¹⁶ along with the Perdew-Burke-Ernzerhof (PBE) generalized gradient approximation (GGA).¹⁷ The GGA plus on-site Coulomb interaction approach (GGA + *U*) were employed with *U* = 5.8 and 7.5 eV for the Ti 3*d* and La 4*f* orbitals, respectively. A kinetic energy cutoff of 450 eV, and a $10 \times 10 \times 1$ *k*-space grid were used. The convergence threshold for the self-consistent-field iteration was set at 10^{-5} eV, and all the atomic positions were fully optimized until the atomic forces were smaller than 0.02 eV/Å. A supercell approach is used to model the HS which contain two symmetrical $(\text{LaO})^{+1}/(\text{TiO}_2)^0$ *n*-type interfaces at $(\text{LAO})_{4.5}/(\text{STO})_{11.5}$ HS.

We first revisited the electronic properties and the 2DEG formation mechanism in the LAO/STO HS. The experimental

^{a)}Email: kesong@ucsd.edu. Tel.: +1-858-534-2514.

lattice constant of STO of 3.905 \AA was used to model the unstrained HS system. The calculated partial density of states (DOS) projected on Ti $3d$ orbitals from three consecutive interfacial TiO_2 layers in the STO substrate is shown in Fig. 1. The 1st, 3rd, and 5th layers of STO was defined as IF-I, IF-III, and IF-V, respectively. Our calculations clearly show that the metallic states are formed in the HS system, and most of the metallic states near the Fermi level come from the 1st TiO_2 layer (IF-I layer) of the STO substrate, along with a small contribution from the 3rd (IF-III) and 5th (IF-V) layers. Further partial DOS analysis indicates that all the other layers away from the interface nearly show an insulating behavior. This means that the mobile charges can move up to ~ 3 unit cells of the STO substrate, showing that the depth of formed 2DEG in the HS system can reach $\sim 10 \text{ \AA}$. Moreover, it is evident that the half-metallic states are formed at the IF-I and IF-III layers, indicating that the partially occupied Ti $3d$ orbitals lead to magnetic moments of $0.38 \mu_B$ and $0.08 \mu_B$ on IF-I and IF-III Ti ions, respectively. Interestingly, these magnetic moments on Ti ions can even cause ferromagnetism in the LAO/STO HS system.^{18,19}

Next, we explored the influence of biaxial strain on the interfacial electronic properties of LAO/STO HS system. We modeled the biaxial strain exerted on the STO by tuning its lattice parameter in the ab -plane. The experimental lattice parameter of STO, 3.905 \AA , is used as a reference point. We started the simulation by taking 0% strain, which means that lattice parameter in the ab -plane is set as 3.905 \AA , and then vary the strain from -3% to $+3\%$ by changing the lattice parameter of STO. The “-” and “+” signs indicate compressive and tensile strains, respectively. To qualitatively show how the electronic properties change with various biaxial strains, we produced the DOS plots of fully relaxed LAO/STO HS systems with strains of -3% (a), -2% (b), -1% (c), $+1\%$ (d), $+2\%$ (e), and $+3\%$ (f) (see Fig. 2). To guarantee a qualitative description of the changing trend for the charge carrier density as the degree of strain, the same cut-off atomic radii taken from the default value of the PBE potentials were used for each system. As mentioned above, the 2DEG of the LAO/STO HS system is primarily composed of Ti $3d$ orbitals. Therefore, we only show the DOS plots of the $3d$ orbitals of Ti atoms near the interfacial region in Fig. 2. Although not shown here, the total DOS plots give

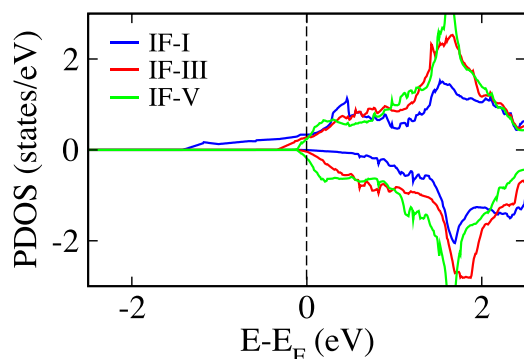


FIG. 1. Calculated Ti $3d$ partial DOS at $(\text{LaO})^{+1}/(\text{TiO}_2)^0$ n -type interface layers for unstrained LAO/STO HS. The Fermi level is indicated by the vertical dashed line at 0 eV. The IF-I, IF-III, and IF-V stand for the 1st, 3rd, and 5th TiO_2 layers of STO, respectively.

similar electronic structure characteristics around the Fermi level. Our calculations indicate that all the HS systems with various strains form metallic states on and near the interfacial region. Surprisingly, the system with -3% compressive strain (Fig. 2(a)) shows the least Ti $3d$ states near the Fermi level, while the system with $+3\%$ tensile strain (Fig. 2(f)) shows the most. When the STO substrate undergoes a strain from -3% to $+3\%$, the density of Ti $3d$ states near the Fermi level increases. This indicates that the charge carrier density of a 2DEG system would increase when a larger tensile strain is exerted on the substrate.

On the one hand, when the HS system undergoes a compressive strain from -1% to -3% , Ti $3d$ gap states on the IF-I layer significantly shrink towards the conduction band and their orbital occupation number decreases. In contrast, Ti $3d$ gap states on the IF-III and IF-V layers substantially extend into the band gap and their occupation number increases. This indicates that, when the compressive strain is applied, more charge is transferred to deeper layers (IF-III and IF-V layers) in the STO substrate. In contrast, when the HS system undergoes a tensile strain from $+1\%$ to $+3\%$, occupation of Ti $3d$ states on the IF-I layer increase, while those of the IF-III and IF-V layers reduce and even disappear. This indicates that, in these tensile-strained systems, the metallicity mainly comes from the IF-I Ti $3d$ orbitals. In particular, for the HS systems with $+2\%$ and $+3\%$ strains (see Figs. 2(e) and 2(f)), the Ti atoms on the IF-III and IF-V layers show insulating behavior and they are non-spin-polarized. This indicates that the 2DEG in these two systems is tightly confined in ab -plane on the 1st layer (IF-I layer) of the STO substrate, with an estimated depth of $\sim 3.9 \text{ \AA}$. Hence, the biaxial strain applied on the STO substrate can significantly influence the spatial extension of the 2DEG along the c -axis.

In order to have a direct view of the spatial extension of the 2DEG along the c -axis, we calculated the charge density projected on the bands forming the 2DEG for LAO/STO HS system with various strains, shown in Fig. 3. The results clearly show that, when a compressive strain is applied on the STO substrate, electrons transferred from the polar $(\text{LaO})^{+1}$ layer to the STO substrate extend to the deeper $(\text{TiO}_2)^0$ layers, i.e., IF-V and IF-VII layers. This indicates that the metallic region spans up to 4.5 unit cells along the c -axis, which weakens the quantum confinement effects of the 2DEG. Hence, the charge carrier density and magnetic moments decrease within the IF-I layers. In contrast, when a tensile strain is applied on the STO substrate, electrons transferred from the polar $(\text{LaO})^{+1}$ layer to the STO substrate are mainly confined at $(\text{TiO}_2)^0$ layers near the interfacial region. In particular, for the HS system with a tensile strain $\geq +2\%$, the interface metallicity stems entirely from the Ti atoms on the IF-I layer, forming an ideal 2DEG.

To obtain a qualitative comparison of the charge carrier density for these HS systems, by integrating the DOS of the occupied Ti $3d$ states on the interface layer, we calculated their occupation number and charge carrier density for each system. The estimated partial occupations of the IF-I Ti $3d$ orbitals are 0.154, 0.164, 0.176, 0.295, 0.316, 0.347, and 0.361 for -3% , -2% , -1% , 0% , $+1\%$, $+2\%$, and $+3\%$ biaxial strains in ab -plane, respectively. The corresponding

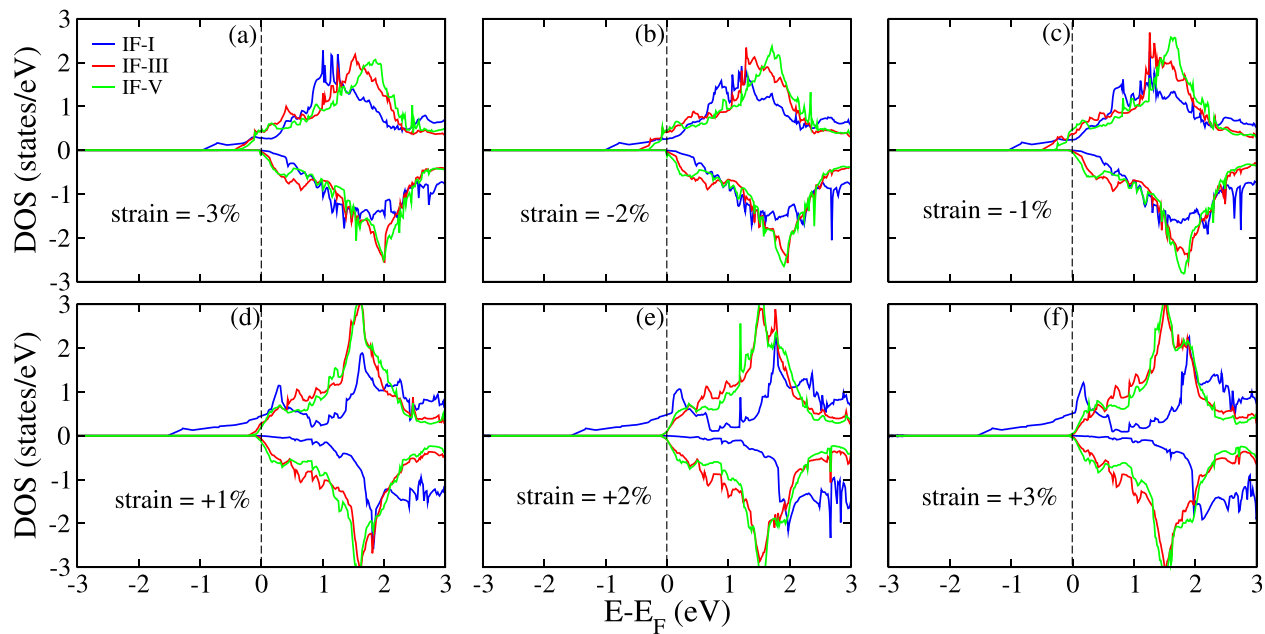


FIG. 2. Calculated Ti 3d partial DOS at $(\text{LaO})^{+1}/(\text{TiO}_2)^0$ n -type interface layers of LAO/STO HS for (a) -3% , (b) -2% , (c) -1% , (d) $+1\%$, (e) $+2\%$, and (f) $+3\%$ strains in the ab -plane. The “ $-$ ” and “ $+$ ” signs indicate compressive and tensile strains, respectively. The Fermi level is indicated by the vertical dashed line at 0 eV.

charge carrier densities for IF-I Ti 3d orbitals are exhibited in Fig. 4(a). Our results show that as the strain is adjusted from -3% to $+3\%$, the charge carrier density increases. In fact, it has been experimentally found by Eom *et al.* that the charge carrier density of the interface layer in the LAO/STO HS system increases when the STO substrate undergoes a strain in the range from about -1.5% to $+0.5\%$.¹⁵ This is consistent with our theoretical calculations. Moreover, in a recent experiment, Moler *et al.* found that the LAO/STO HS system exhibits an enhanced electron transport property when the STO substrate has a tetragonal structure with a lengthened axis along the interface plane.²⁰ The lengthened axis along the ab -plane corresponds to our theoretical model with a tensile strain, which shows a higher charge carrier density. Therefore, our theoretical calculations clearly reveal the role of changing substrate lattice along the interface plane in tailoring interfacial charge carrier density of the STO-based HS systems, which gives a good explanation for the enhanced conductivity in the experiment of Moler *et al.* However, we also point out that in the experiment of Eom *et al.*, when the 1.1% and 1.6% tensile strains are exerted on

the STO substrate, the charge carrier density of the LAO/STO HS system has a surprising sharp decrease,¹⁵ which is different from our theoretical prediction. This discrepancy can most likely be attributed to a more complex interface structure formed in the experiment. This discrepancy, however, is not against our conclusion of the strain dependence on the interfacial electronic properties because it probably involves more complex interface structure beyond the strained model.

Next, we found that the magnetic moments at and near the interfacial region also show substantial changes (see Fig. 4(b)). When the STO substrate undergoes a strain from -3% to $+3\%$, the magnetic moments of the Ti atoms in the IF-I layer significantly increase, while those in the IF-III and IF-V layers decrease. This is because less charge is transferred from the IF-I layer to the deep IF-III and IF-V layers. Hence, more robust magnetism of the 2DEG is expected to occur in HS systems with larger tensile strains.

The trend of charge carrier density and magnetic moment of the 2DEG with biaxial strain can be understood from the structural distortion of the TiO_6 unit on the

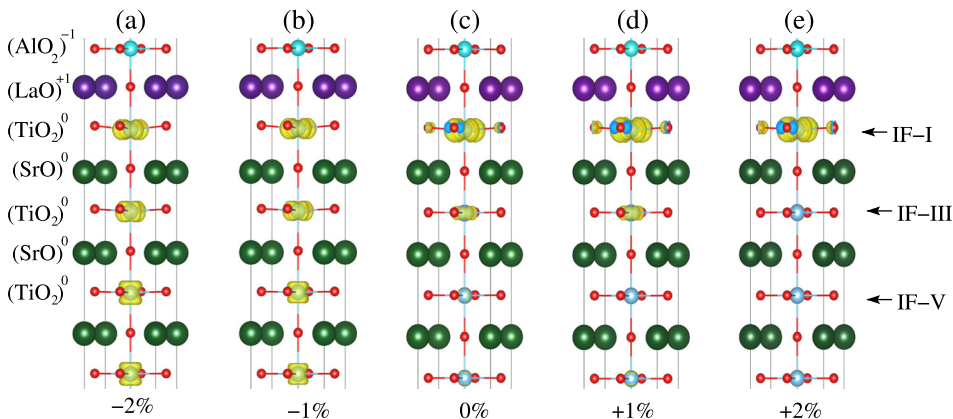


FIG. 3. Charge density projected on the bands forming the 2DEG of LAO/STO HS for (a) -2% , (b) -1% , (c) 0% , (d) $+1\%$, and (e) $+2\%$ strain in ab -plane. The “ $-$ ” and “ $+$ ” signs indicate compressive and tensile strains, respectively. The same iso-value of 0.0038 is used to produce the charge density plots.

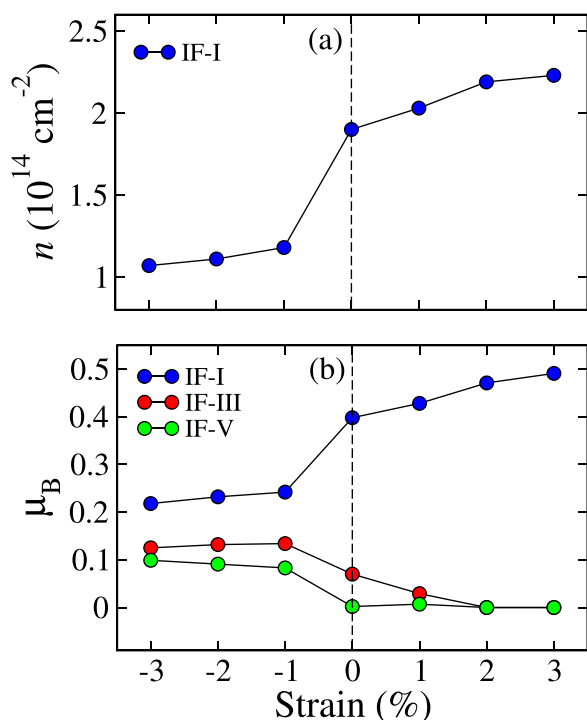


FIG. 4. Calculated (a) charge carrier density and (b) magnetic moments with respect to strain for LAO/STO HS.

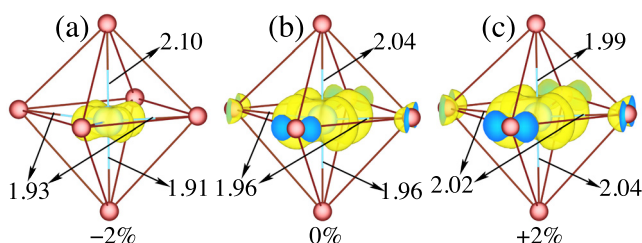


FIG. 5. Locally distorted TiO₆ octahedra at with calculated three-dimensional charge density projected on the bands forming 2DEG for: -2% (a), 0% (b), and +2% (c) strains at LAO/STO HS.

interface. Therefore, we plotted the locally distorted TiO₆ octahedra and projected charge density on the bands forming the interfacial 2DEG for -2% (a), 0%, and +2% strain systems in Fig. 5. In the regular octahedral crystal field, the Ti 3d states are split into triply t_{2g} (d_{xy} , d_{xz} , and d_{yz}) and doubly e_g ($d_{3z^2-r^2}$ and $d_{x^2-y^2}$) degenerate states. When a compressive (tensile) strain is applied in the ab -plane of the STO substrate, the TiO₆ octahedron on the interface is elongated (shortened) along the c -axis, i.e., perpendicular to the ab -plane. This means that the O_h symmetry of the local TiO₆ unit is reduced to D_{4h} , and thus the degeneracy of the Ti 3d orbitals is degraded. The t_{2g} states are further split into d_{xy} and doubly (d_{xz} , d_{yz}) degenerate states. The partial DOS analysis shows that the metallic states and magnetic moments are mainly induced by the d_{xy} orbitals in the ab -plane. When a tensile strain is applied on the STO substrate, the Ti-O bond length in the ab -plane increases, see Fig. 5(c). This makes the d_{xy} orbitals of Ti atoms on the IF-I layer hold more electrons, and thus the electrons transferred from the polar (LaO)⁺ layer are concentrated on the IF-I layer. On the

contrary, when a compressive strain is applied on the STO substrate, the Ti-O bond length in the ab -plane decreases (Fig. 5(a)), and the d_{xy} orbitals of Ti atoms on the IF-I layer cannot hold all the electrons, and hence the remaining electrons will transfer to deeper IF-III, IF-V, and even IF-VII layers.

In summary, first-principles electronic structure calculations were employed to explore the possibility of enhancing the interfacial conductivity and spatial charge confinement of LAO/STO HS system via strain engineering. Our results revealed two important conclusions. (1) The LAO/STO with a tensile strain can lead to more occupied Ti 3d gap states near the interfacial region and thus higher charge carrier density with respect to the unstrained system. (2) The 2DEG in the LAO/STO HS system can be tightly confined in the interfacial layer when a moderate tensile strain is exerted, which further enhances the interfacial charge carrier density and magnetic moments.

This work was supported by start-up funds from the University of California, San Diego. This work used the Extreme Science and Engineering Discovery Environment (XSEDE), which is supported by National Science Foundation grant number ACI-1053575.

- ¹A. Ohtomo and H. Y. Hwang, *Nature* **427**, 423 (2004).
- ²N. Nakagawa, H. Y. Hwang, and D. A. Muller, *Nat. Mater.* **5**, 204 (2006).
- ³J. Mannhart and D. G. Schlom, *Science* **327**, 1607 (2010).
- ⁴S. Thiel, G. Hammerl, A. Schmehl, C. W. Schneider, and J. Mannhart, *Science* **313**, 1942 (2006).
- ⁵C. Cen, S. Thiel, G. Hammerl, C. W. Schneider, K. E. Andersen, C. S. Hellberg, J. Mannhart, and J. Levy, *Nat. Mater.* **7**, 298 (2008).
- ⁶P. Delugas, A. Filippetti, V. Fiorentini, D. I. Bilc, D. Fontaine, and P. Ghosez, *Phys. Rev. Lett.* **106**, 166807 (2011).
- ⁷S. Okamoto and A. J. Millis, *Nature* **428**, 630 (2004).
- ⁸S. A. Pauli and P. R. Willmott, *J. Phys.: Condens. Matter* **20**, 264012 (2008).
- ⁹R. Pentcheva and W. E. Pickett, *J. Phys.: Condens. Matter* **22**, 043001 (2010).
- ¹⁰J. M. Rondinelli and N. A. Spaldin, *Adv. Mater.* **23**, 3363 (2011).
- ¹¹A. Dubroka, M. Rössle, K. W. Kim, V. K. Malik, L. Schultz, S. Thiel, C. W. Schneider, J. Mannhart, G. Herranz, O. Copie, M. Bibes, A. Barthélémy, and C. Bernhard, *Phys. Rev. Lett.* **104**, 156807 (2010).
- ¹²K. Yang, W. Setyawan, S. Wang, M. B. Nardelli, and S. Curtarolo, *Nat. Mater.* **11**, 614 (2012).
- ¹³A. Savoia, D. Paparo, P. Perna, Z. Ristic, M. Salluzzo, F. Miletto Granozio, U. Scotti di Uccio, C. Richter, S. Thiel, J. Mannhart, and L. Marrucci, *Phys. Rev. B* **80**, 075110 (2009).
- ¹⁴Z. Q. Liu, C. J. Li, W. M. Lü, X. H. Huang, Z. Huang, S. W. Zeng, X. P. Qiu, L. S. Huang, A. Annadi, J. S. Chen, J. M. D. Coey, T. Venkatesan, and Ariando, *Phys. Rev. X* **3**, 021010 (2013).
- ¹⁵C. W. Bark, D. A. Felker, Y. Wang, Y. Zhang, H. W. Jang, C. M. Folkman, J. W. Park, S. H. Baek, H. Zhou, D. D. Fong, X. Q. Pan, E. Y. Tsybmal, M. S. Rzchowski, and C. B. Eom, *Proc. Natl. Acad. Sci.* **108**, 4720 (2011).
- ¹⁶G. Kresse and J. Furthmüller, *Phys. Rev. B* **54**, 11169 (1996).
- ¹⁷J. P. Perdew, K. Burke, and M. Ernzerhof, *Phys. Rev. Lett.* **77**, 3865 (1996).
- ¹⁸J. S. Lee, Y. W. Xie, H. K. Sato, C. Bell, Y. Hikita, H. Y. Hwang, and C. C. Kao, *Nat. Mater.* **12**, 703 (2013).
- ¹⁹L. Li, C. Richter, J. Mannhart, and R. C. Ashoori, *Nat. Phys.* **7**, 762 (2011).
- ²⁰B. Kalisky, E. M. Spanton, H. Noad, J. R. Kirtley, K. C. Nowack, C. Bell, H. K. Sato, M. Hosoda, Y. Xie, Y. Hikita, C. Woltmann, G. Pfanzelt, R. Jany, C. Richter, H. Y. Hwang, J. Mannhart, and K. A. Moler, *Nat. Mater.* **12**, 1091 (2013).